First Experimental Realization of the Dirac Oscillator

J. A. Franco-Villafañe,[1] E. Sadurní,[2] S. Barkhofen,[3] U. Kuhl,[4] F. Mortessagne,[4] and T. H. Seligman[1,5]

[1]*Instituto de Ciencias Físicas, Universidad Nacional Autónoma de México, Avenida Universidad s/n, 62210 Cuernavaca, México*
[2]*Instituto de Física, Benemérita Universidad Autónoma de Puebla, Apartado Postal J-48, 72570 Puebla, México*
[3]*Fachbereich Physik, Philipps-Universität Marburg, Renthof 5, 35032 Marburg, Germany*
[4]*Laboratoire de Physique de la Matière Condensée, Université de Nice-Sophia Antipolis, CNRS, UMR 7336 Parc Valrose—06108 Nice, France*
[5]*Centro Internacional de Ciencias, 62210 Cuernavaca, México*

(Received 6 June 2013; published 24 October 2013)

We present the first experimental microwave realization of the one-dimensional Dirac oscillator, a paradigm in exactly solvable relativistic systems. The experiment relies on a relation of the Dirac oscillator to a corresponding tight-binding system. This tight-binding system is implemented as a microwave system by a chain of coupled dielectric disks, where the coupling is evanescent and can be adjusted appropriately. The resonances of the finite microwave system yield the spectrum of the one-dimensional Dirac oscillator with and without a mass term. The flexibility of the experimental setup allows the implementation of other one-dimensional Dirac-type equations.

DOI: 10.1103/PhysRevLett.111.170405 PACS numbers: 03.65.Pm, 07.57.Pt, 41.20.−q, 73.22.Pr

The relativistic version of the harmonic oscillator has been touched upon occasionally [1,2] but became a widely used model for relativistic equations with the appearance of the seminal paper [3]. Originally, it was known as the Dirac oscillator (DO) [4,5]. Indeed, since then, the number of papers using this model has increased rapidly, mainly in mathematical physics [6–19], but also in nuclear physics [20–22], subnuclear physics [23,24], and quantum optics [25–28]. In mathematical physics, it has become the paradigm for the construction of covariant quantum models with some well determined nonrelativistic limit but has also attracted much attention in the environment of exactly solvable models and symmetries; it is amusing to mention that even the Higgs symmetry has been considered in this context [29].

While this model is a paradigm of mathematical physics, it does not describe a known physical system, as is the case for the Dirac equation for the hydrogen atom. Thus, an experimental realization by other means is highly desirable. There are two proposals to realize analogue experiments: one in the realm of quantum optics [26–28] and the other one using a classical microwave setup [30]. In this Letter, we shall present a microwave realization for the 1D DO. Beyond its intrinsic interest, the experiment is also a starting point for further experimental exploration of Dirac-like equations.

We will mainly follow the proposition of Ref. [30] but use a slightly different mechanism to appropriately take into account the finiteness of the experimental system. The experimental idea is based on a mapping of the DO to a tight-binding model with dimers. In this model, it is important that only nearest neighbor interactions are present. It consists of a chain of coupled disks with a high index of refraction sandwiched between two metallic plates. The coupling constants between the disks have to be adjusted properly to obtain a spectrum which is equivalent to the DO spectrum. This setup has been used to investigate the Dirac points [31], disorder effects [32], and topological transitions in graphene [33]. We start with a short introduction to the DO and its relation to a tight-binding Hamiltonian with nearest neighbor coupling only. Thereafter, we introduce the experimental setup and present the experimental results.

Dirac oscillator.—The system that we now call the DO was proposed more than 20 years ago [3,34–37], and its properties and possible applications have been studied extensively. The original formulation was presented in Hamiltonian form. Covariance was easily achieved, and the physicality of such a system could be attained by means of a Pauli coupling [3]. In the present Letter, we will use the $1+1$-dimensional version of the Dirac oscillator [4], which can be treated analogously and yields a two-component spinless structure.

The system in question can be conceived in its simplest form by writing the corresponding Hamiltonian as a function of the spectrum generating algebra. Let a, $a^\dagger$ be the ladder operators of a nonrelativistic harmonic oscillator and $\sigma_\pm = \sigma_x \pm i\sigma_y$ the creation and annihilation operators of spin $1/2$ in terms of Pauli matrices. The $1+1$-dimensional DO Hamiltonian is

$$H = \sigma_+ a + \sigma_- a^\dagger + \mu\sigma_z, \tag{1}$$

where the spectrum is given by

$$\epsilon_{\pm,n} = \pm\sqrt{n+\mu^2}, \tag{2}$$

where the sign denotes particles and antiparticles. The dimensionless commutator $[a, a^\dagger] = 1$ ensures that for a particle of mass m and an oscillator of frequency ω, we

have $\mu = \sqrt{mc^2/\hbar\omega}$. Thus, in the appropriate units, μ gives the mass of the particle directly, and the time variable scales as $t \mapsto \sqrt{\omega mc^2/\hbar}t$. In a certain limit, the DO can also be reduced to the Weyl equation with a linear potential; thus, one may call this system even a Weyl oscillator. Taking $m \to 0$ and leaving $m\omega = \text{const} \neq 0$ leads to $\mu \to 0$, and the following massless Hamiltonian

$$H = \sigma_+ a + \sigma_- a^\dagger, \tag{3}$$

with the simplified spectrum

$$\epsilon_n = \pm\sqrt{n}. \tag{4}$$

Note here that for $n = 0$, there is a double degeneracy, where one of the states is given by $|-, 0\rangle$. Both Hamiltonians (2) and (3) can be described within a tight-binding model with dimers.

Description as a tight-binding model.—The eigenvalue problem resulting from the Hamiltonian (1) can be written as two coupled tight-binding equations of the form

$$\sqrt{n+1}\,\psi^-_{n+1} + \mu\psi^+_n = \epsilon_n \psi^+_n, \tag{5}$$

$$\sqrt{n}\,\psi^+_{n-1} - \mu\psi^-_n = \epsilon_n \psi^-_n, \tag{6}$$

where $\psi^\pm_n$ is the atomic wave function of the nth dimer and the superscripts $+$ and $-$ indicate sites of types A and B (see also Fig. 1). In our previous work [30], we have established that this model can be emulated in a one-dimensional chain with nearest neighbor interactions where the spin ($\pm$ superscripts in the equations above) can be represented by A and B sites in a linear chain. By defining the new operators

$$b = \Delta(1 + a), \qquad b^\dagger = \Delta(1 + a^\dagger), \tag{7}$$

the Hamiltonian for a tight-binding chain of two species can be written as

$$H_{\text{chain}} = \sigma_+ b + \sigma_- b^\dagger + \mu\sigma_z, \tag{8}$$

and μ is now the energy difference between the resonances sitting upon A and B sites, giving rise to a spectral gap.

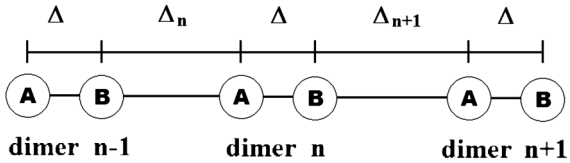

FIG. 1. A chain of resonators in dimeric configuration, with atoms of types A and B. The index n stands for the dimer number, Δ is the coupling between elements of the same dimer (intradimer coupling, kept constant throughout the array), and Δ_n is the coupling between the right end of dimer n and the left end of dimer $n + 1$ (interdimer coupling). Have in mind that here we present the couplings only, later on $\Delta \leq \Delta_n$, which means that in the experiment, the intradimer distance is the largest distance in the chain.

The constant Δ is nothing else than the coupling between two sites, and the spectrum of the system can be extracted by virtue of the algebraic relation $[b, b^\dagger] = \Delta^2$. As before, we have

$$\epsilon_n = \pm\sqrt{\Delta^2 n + \mu^2}. \tag{9}$$

The map between the DO and the coupled linear chain of two species is therefore quite natural. Finally, we can see that the resulting array comprises dimers AB; e.g., site A is always equally coupled to site B by Δ independently on n, whereas the coupling between the dimers Δ_n has to follow a specific law derived below. The requirements for a realization of b, $b^\dagger$, on the other hand, introduce the following restrictions: For the interdimer coupling, $\Delta_n = \Delta\sqrt{n}$.

An appropriate cutoff.—Until now, we assumed a semi-infinite array which terminates at one end with the value $\Delta_0 = 0$ (no more dimers to the left). Therefore, couplings of the form $\sqrt{n}$ range from 0 to $\lim_{n\to\infty}\Delta_n = \infty$. However, experimentally accessible couplings always have an upper limit Δ_{sup} determined by the physical situation and such a restriction introduces a natural cutoff in the array by means of the relation $\Delta_{\text{sup}} = \Delta\sqrt{n_{\text{sup}}}$. Thus, we arrive at a finite chain with a total number $2n_{\text{sup}}$ of sites.

A previously proposed finite realization [30], although well conceived for the infinite case, did not take into account cutoff effects appropriately. Any configurations of type $b = \Delta a + \delta$ for arbitrary δ fulfills the algebraic relations, but to keep edge effects small, δ must be smaller than any other coupling in the system. Choosing $\delta = \Delta$ is sufficient for this purpose. The preferred tight-binding models are such that the successive couplings are increased until a maximal coupling is reached, which is in contrast with the previous proposition.

The generation of mass.—Our scheme so far contemplates the appearance of a spectral gap corresponding to a finite mass in the DO to result from an inherent asymmetry within the dimer; i.e., A and B have different eigenenergies. This produces the term $\mu\sigma_z$ in the Hamiltonian [Eq. (1)]. However, in practice, an alternate option to generate a gap occurs due to finite size effects: We choose the smallest interdimer coupling to be slightly smaller, rather than equal to the intradimer coupling, i.e., $\Delta' \gtrsim \Delta_{\text{min}}$. Numerical inspection of the tight-binding model shows that, while a gap opens, the effects on the relative position of the eigenvalues on both sides of the gap have finite size errors similar to the ones in the gapless case. Note that the gap depends on the number of sites and vanishes as this number goes to infinity; therefore, a large array will not describe a DO with mass, in compliance with the chiral symmetry of the system [38]. Yet, for finite sizes, we do get the desired spectrum and we can make appropriate approximations or numerical calculations in the tight-binding model to explain this satisfactorily. Nevertheless, we suggest to adapt the gap size to the experimental one rather than to get it from a tight-binding model, as there will

always remain discrepancies between the model and the experiment, which are entirely unrelated to the DO. If we wish to take advantage of this finite size effect, we should thus replace Eq. (8) by

$$\epsilon_n = \pm\sqrt{\Delta^2 n + \mu_{\mathrm{exp}}^2}, \tag{10}$$

where μ_{exp} refers to the parameter determined by the experiment.

Experimental results.—For the experimental realization of the DO, we use the techniques that have been developed to investigate the band structure of graphene [31–33]. The realization of the DO is achieved as tight-binding system with nearest neighbor coupling and small higher order ones. A set of identical dielectric cylindrical disks (5 mm height, 4 mm radius, and a refractive index of about 6) is placed between two metallic plates (see Fig. 2). Close to one disk, we placed a kink antenna connected to a vectorial network analyzer, allowing us to excite both transverse magnetic and transverse electric (TE) modes. The individual disks have an isolated TE resonance at 6.65 GHz. We restrict our investigation to frequencies around this value, where each disk contributes only one resonance. The electromagnetic field for this TE mode is mostly confined within the disks and spreads evanescently outside. A sketch of the experimental setup is shown in Fig. 2, and a detailed description is presented in Ref. [32].

In contrast to Refs. [31,32], we adjusted the height between the two plates to $h = 13$ mm, to reduce the higher order neighbor couplings. The coupling parameter Δ between two adjacent disks depends on the distance between centers of the disks d and can be given in terms of a modified Bessel function $|K_0|^2$, as described in Refs. [31,32]. Thus, by changing the distance between disks, one changes the interdisk couplings and obtains the 1D DO.

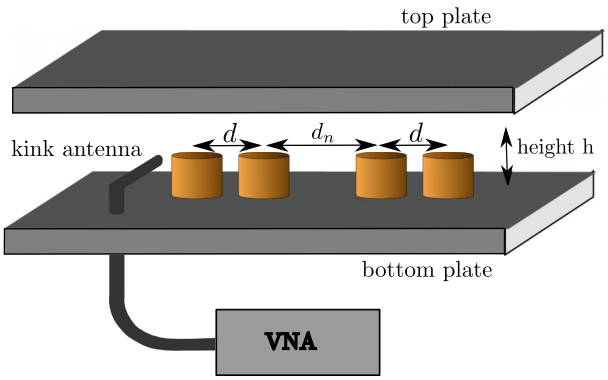

FIG. 2 (color online). Disks with a high index of refraction are placed between two metallic plates as a chain with center to center distances d_n or d. The microwaves are induced by a vector network analyzer (VNA) via a microwave cable and a kink antenna.

For the sake of simplicity, let us assume an exponential law which is a good approximation of the coupling in terms of the distance in the range of interest. Then, the distances d_n between the dimers in the massless case are given by

$$d_n = -\frac{1}{\gamma}\ln\left(\frac{\Delta_n}{\Delta_K}\right) = -\frac{1}{\gamma}\ln\left(\frac{\Delta\sqrt{n}}{\Delta_K}\right). \tag{11}$$

The intradimer distance is d, and we chose $d_1 = d$. The distances between the dimers are decreasing monotonically; thus, the smallest possible distance d_{inf} determined by the diameter of the disks d_D defines the largest possible coupling Δ_{sup} and the largest allowable number of dimers n_{sup}, giving the largest admissible size of our dimer chain. The number of energy levels is therefore equal to $2n_{\mathrm{sup}}$. The eigenfrequencies for the 1D DO without mass are then given by

$$\nu_n = \nu_c \pm \Delta\sqrt{n}, \tag{12}$$

where ν_c is the eigenfrequency of a single disk. We used an intradimer distance d of 13, 14, and 15 mm and chains of 12, 18, 24, and 30 disks. In Fig. 3, we show the reflection spectra for $d = 13$ mm and 30 disks for two different antenna positions. The height of the resonances depends on the antenna site, as it is proportional to the intensity of the wave function at the disk. By measuring at different sites, it is possible to extract all resonance positions. The vertical lines correspond to the theoretical predictions, and a good agreement is found. Deviations increase at the edges of the spectrum, as designed by the choice of the cutoff.

We now investigate the dependence on the chain length. The measured eigenfrequencies as a function of the mode number are shown in Fig. 4. The continuous curve corresponds to the analytical prediction [Eq. (12)]. As the number of dimers increases, we find that the low levels

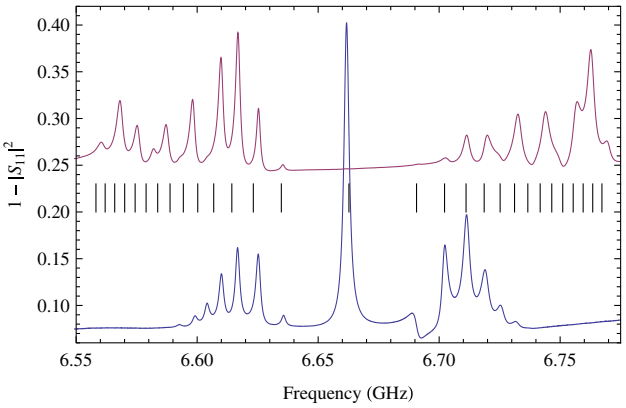

FIG. 3 (color online). Reflection spectra of a Dirac oscillator without mass for a 15 dimer chain with minimal dimer distance of $d_{\mathrm{min}} = 13$ mm. The upper spectrum (up-shifted) is measured at the 15th disk, whereas the lower is measured at the 3rd disk. The vertical lines indicate the predicted resonance positions from Eq. (12) with $\Delta = 0.023$ GHz.

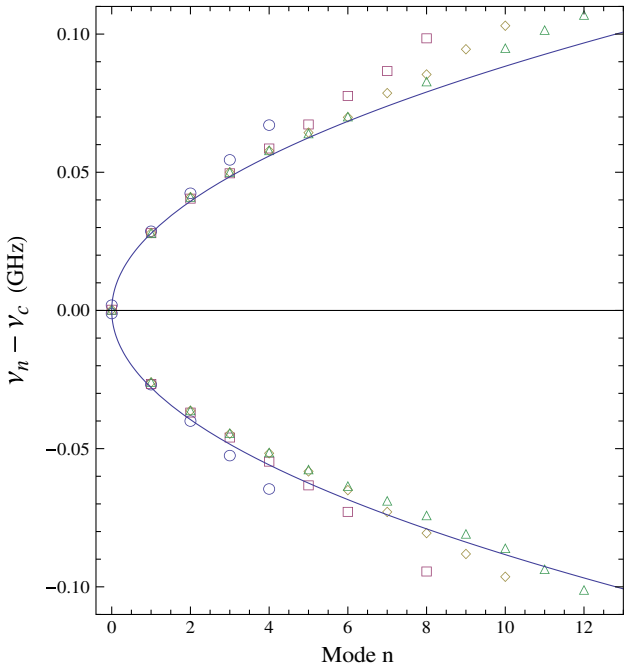

FIG. 4 (color online). Dirac oscillator without mass for an intradimer distance of 13 mm. The continuous curve corresponds to the analytical prediction [Eq. (12)]. The symbols correspond to different numbers of dimers: 6 dimers (circles), 9 dimers (squares), 12 dimers (diamonds), and 15 dimers (triangles).

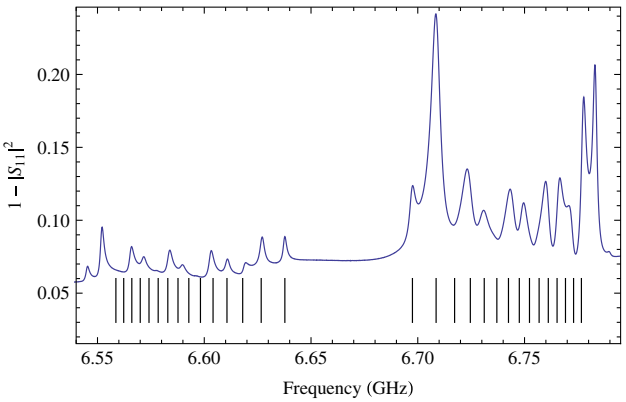

FIG. 5 (color online). Reflection spectrum of a Dirac oscillator with mass for a 15 dimer chain, where the intradimer distance of 10 mm and the interdimer distance of $d_{\min} = 10.81$ mm. The vertical lines indicate the predicted resonance positions from Eq. (12) with $\mu = 1.066$ GHz and $\Delta = 0.028$ GHz.

are best reproduced by the theoretical curve [Eq. (12)], and the point of departure from theory moves further away from the center of the spectrum as the number of dimers increases. For dimer distances of 14 and 15 mm, we got similar results. Thus, we experimentally measured the spectrum of the Dirac oscillator without mass in a finite approximation.

As we only have disks of the same type, meaning having approximately the same resonance frequency, we cannot directly generate the 1D DO with mass as originally introduced. But, as mentioned above, for a finite chain, one can introduce a mass term by setting the intradimer coupling Δ' larger than the smallest coupling between the dimers $\Delta_{\min}$. Thus, we only have to set the intradimer distance d to be smaller than the maximal interdimer distance d_1. We used a chain of 15 dimers with an initial interdimer distance $d_1 = 15$ mm and a smallest interdimer distance $d_{14} = d_{\min} \approx 10.81$. As intradimer distances d, we choose 10, 11, and 12 mm. In Fig. 5, we present the reflection spectra and the theoretical prediction [Eq. (2)] for $d = 10$ mm. We observe the expected gap at the center and find a good agreement for the resonances close to the gap. Again, the outer resonances show larger deviations. Next, we removed step by step the last dimer, thus increasing the minimal interdimer distance $d_{\min}$ starting with $d_{\inf}$.

In Fig. 6, the resonances for different chain lengths are shown. We observe a good agreement for the upper spectrum with Eq. (2). The two bands behave slightly differently; especially, their width is different, due to the second nearest neighbor couplings, as was also observed in square and graphene lattices [39]. Furthermore, the gap is observed to increase monotonically with $d_{\min}$.

In conclusion, we have experimentally realized the 1D DO based on the correspondence of the DO to a tight-binding model. Within this model, effects of finite size are

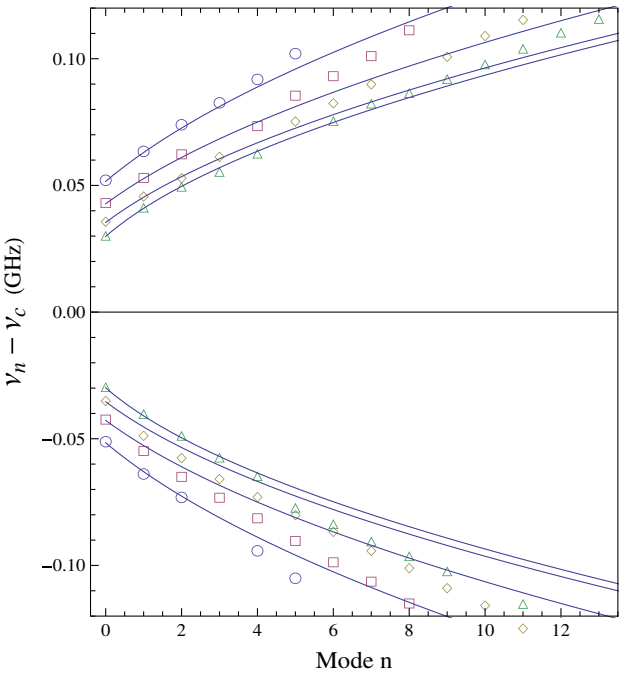

FIG. 6 (color online). Dirac oscillator with mass for a different number of dimers, where the last dimers are removed. The intradimer distance is $d = 10$ mm. Displayed are 6 ($d_{\min} \approx 12.32$ mm, circles), 9 ($d_{\min} \approx 11.61$ mm, squares), 12 ($d_{\min} \approx 11.15$ mm, diamonds), and 15 ($d_{\min} \approx 10.81$ mm, triangles). Additionally, the corresponding theoretical curves resulting from Eq. (9) are plotted as solid lines.

small at the center of the spectrum. Furthermore, we have produced a gap in the spectrum which can be interpreted as the mass of the fermion. This was done by a distortion that applies only to finite arrays, as the infinite limit of the system makes such a gap vanish. We hope for the future to investigate wave functions and pulse propagation as well. Both are accessible for the setup if one uses a movable antenna with an additionally fixed antenna and measures the transmission [33,39]. Additionally, we would like to realize a 2D DO, as mentioned in Ref. [30]. The model assumes a logarithmically deformed hexagonal lattice with only nearest neighbor couplings. To respect this coupling condition, a realization of the 2D DO is not possible with our distance-coupling relation. However, microwave graphs seems to be a promising candidate [40,41].

T. H. S., J. A. F. V., and S. B. thank the University of Nice for the hospitality during several long term visits at the LPMC. T. H. S. and J. A. F. V. acknowledge CONACyT Project No. 79613, PAPIIT-UNAM Project No. IG101113, and PAEP-UNAM for financial support. E. S. acknowledges support from PROMEP Project No. 103.5/12/4367.

[1] D. Itô, K. Mori, and E. Carriere, Nuovo Cimento A **51**, 1119 (1967).
[2] P. A. Cook, Nuovo Cimento **1**, 149 (1971).
[3] M. Moshinsky and A. Szczepaniak, J. Phys. A **22**, L817 (1989).
[4] E. Sadurní, AIP Conf. Proc. **1334**, 249 (2010).
[5] J. M. Torres, E. Sadurní, and T. H. Seligman, AIP Conf. Proc. **1323**, 301 (2010).
[6] M. Hamzavi, M. Eshghi, and S. M. Ikhdair, J. Math. Phys. (N.Y.) **53**, 082101 (2012).
[7] C.-K. Lu and I. F. Herbut, J. Phys. A **44**, 295003 (2011).
[8] S. Zarrinkamar, A. A. Rajabi, and H. Hassanabadi, Ann. Phys. (Amsterdam) **325**, 2522 (2010).
[9] Y. Chargui, A. Trabelsi, and L. Chetouani, Phys. Lett. A **374**, 2907 (2010).
[10] A. Bermudez, M. A. Martin-Delgado, and A. Luis, Phys. Rev. A **77**, 063815 (2008).
[11] D. A. Kulikov, R. S. Tutik, and A. P. Yaroshenko, Phys. Lett. B **644**, 311 (2007).
[12] A. S. de Castro, P. Alberto, R. Lisboa, and M. Malheiro, Phys. Rev. C **73**, 054309 (2006).
[13] A. C. Alhaidari, H. Bahlouli, and A. Al-Hasan, Phys. Lett. A **349**, 87 (2006).
[14] C. Quesne and V. M. Tkachuk, J. Phys. A **38**, 1747 (2005).
[15] C. L. Ho and P. Roy, Ann. Phys. (Amsterdam) **312**, 161 (2004).
[16] R. Lisboa, M. Malheiro, A. S. de Castro, P. Alberto, and M. Fiolhais, Phys. Rev. C **69**, 024319 (2004).
[17] A. D. Alhaidari, J. Phys. A **34**, 9827 (2001).
[18] A. D. Alhaidari, Phys. Rev. Lett. **87**, 210405 (2001).
[19] J. Benítez, R. P. Martínez y Romero, H. N. Núñez-Yépez, and A. L. Salas-Brito, Phys. Rev. Lett. **64**, 1643 (1990).
[20] J. Munarriz, F. Dominguez-Adame, and R. P. A. Lima, Phys. Lett. A **376**, 3475 (2012).
[21] J. Grineviciute and D. Halderson, Phys. Rev. C **85**, 054617 (2012).
[22] A. Faessler, V. I. Kukulin, and M. A. Shikhalev, Ann. Phys. (Amsterdam) **320**, 71 (2005).
[23] Y. X. Wang, J. Cao, and S. J. Xiong, Eur. Phys. J. B **85**, 237 (2012).
[24] E. Romera, Phys. Rev. A **84**, 052102 (2011).
[25] V. V. Dodonov, J. Opt. B **4**, R1 (2002).
[26] A. Bermudez, M. A. Martin-Delgado, and E. Solano, Phys. Rev. Lett. **99**, 123602 (2007).
[27] L. Lamata, J. León, T. Schätz, and E. Solano, Phys. Rev. Lett. **98**, 253005 (2007).
[28] S. Longhi, Opt. Lett. **35**, 1302 (2010).
[29] F.-L. Zhang, B. Fu, and J.-L. Chen, Phys. Rev. A **80**, 054102 (2009).
[30] E. Sadurní, T. Seligman, and F. Mortessagne, New J. Phys. **12**, 053014 (2010).
[31] U. Kuhl, S. Barkhofen, T. Tudorovskiy, H.-J. Stöckmann, T. Hossain, L. de Forges de Parny, and F. Mortessagne, Phys. Rev. B **82**, 094308 (2010).
[32] S. Barkhofen, M. Bellec, U. Kuhl, and F. Mortessagne, Phys. Rev. B **87**, 035101 (2013).
[33] M. Bellec, U. Kuhl, G. Montambaux, and F. Mortessagne, Phys. Rev. Lett. **110**, 033902 (2013).
[34] M. Moshinsky, G. Loyola, A. Szczepaniak, C. Villegas, and N. Aquino, in *Rio de Janeiro 1989, Relativistic Aspects of Nuclear Physics* (World Scientific, Singapore, 1990), p. 271.
[35] M. Moshinsky, G. Loyola, and C. Villegas, in *Group Theoretical Methods in Physics*, edited by V. Dodonov and V. Man'ko, Lecture Notes in Physics Vol. 382 (Springer, Berlin, 1991), p. 339.
[36] M. Moshinsky, G. Loyola, and A. Szczepaniak, in *J J Giambiagi Festschrift*, edited by H. Falomir (World Scientific, Singapore, 1991).
[37] M. Moshinsky and Y. Smirnov, *Proceedings of the Rio de Janeiro International Workshop on Relativistic Aspects of Nuclear Physics* (Hardwood Academic, Amsterdam, 1996).
[38] G. Semenoff, Phys. Scr. **T146**, 014016 (2012).
[39] M. Bellec, U. Kuhl, G. Montambaux, and F. Mortessagne, Phys. Rev. B **88**, 115437 (2013).
[40] O. Hul, S. Bauch, P. Pakoñski, N. Savytskyy, K. Życzkowski, and L. Sirko, Phys. Rev. E **69**, 056205 (2004).
[41] O. Hul, O. Tymoshchuk, S. Bauch, P. Koch, and L. Sirko, J. Phys. A **38**, 10 489 (2005).